JOURNAL OF APPLIED ELECTROCHEMISTRY 20 (1990) 139–144

Electrochemical and photoelectrochemical behaviour of passivated niobium electrodes during hydrogen evolution

W. A. BADAWY

Department of Chemistry, Faculty of Science, University of Cairo, Giza, Egypt

Received 22 February 1989; revised 1 June 1989

The electrochemical and photoelectrochemical behaviour of niobium electrodes passivated in 0.5 M H_2SO_4 and 1 M HNO_3 has been investigated. High intensity pulse lasers were used as light sources. This technique allows photoelectrochemical measurements with light wavelengths smaller than the band gap of the semiconducting passive film. The donor concentration and the flat band potential of the passive films were calculated from capacity measurements. The effect of cathodic hydrogen evolution on the behaviour of the oxide film formed was found to depend on the time of the cathodic treatment of the electrode. The results showed that the behaviour of the passive film formed on niobium in nitric acid is different from that formed in sulphuric acid. The calculated donor concentrations and the extrapolated flat band potentials indicate that the nature of the passive film depends on the formation medium. The adsorption of hydrogen on the passivated Nb-electrode up to a time limit of 1 ms could be traced using photocharge measurements with excitation energies less than the band gap energy of the semiconducting oxide film.

1. Introduction

Many investigations have been devoted to the production of corrosion resistant materials which can be used in many industrial applications [1, 2]. Niobium, as a valve metal, is known to form stable oxide films in aqueous media [3]. The metal has been subjected to extensive studies, most of which were concerned with the kinetics of the oxide film formation [4–11]. Few studies, however, have been directed towards the stability of the oxide film formed on niobium in aggressive media [12–14]. The passive film on the metal was reported to behave as a weakly dissociated extrinsic semiconductor [15]. It consists mainly of amorphous or glassy Nb_2O_5 [3, 16–18] with a density of 4.74 g cm^{-3} [19] and a static dielectric constant of 45 [3]. It has a high concentration of oxygen vacancies (around 10^{19} cm^{-3}), which act as donor states [20, 21]. For the band gap of Nb_2O_5 crystals a value of 3.4 eV was reported [21, 22].

In most investigations high-voltage anodized niobium was used. The low-voltage passive behaviour of the metal and its photoelectrochemical properties, especially in aggressive and industrially commonly used media, like HNO_3, seems to have been little studied. The great demand for stable materials for use in chemical process units and the application of valve metals to the electrochemical methods recently introduced into the Purex process for minimization of waste [23] makes passivation of niobium and its behaviour during hydrogen evolution an interesting case for further investigation.

As reported previously [24, 25], it is possible to detect small photocurrents on semiconducting passive films formed on metals by the use of high intensity pulse lasers. These light sources even allow investigations with light wavelengths smaller than the band gap of the semiconducting passive film.

The present study reports on the behaviour of the passive film formed on niobium in nitric acid solutions and compares it with the behaviour of the metal passivated in sulphuric acid. The effect of the cathodic hydrogen evolution on the space charge characteristics and the photoelectrochemical behaviour of the passivated electrode is also reported.

2. Experimental

The photocurrent measurements were carried out in a darkened room with a pulsed dye laser to illuminate the electrode surface. The technique used makes possible the simultaneous recording of the cell current and the photocurrent at the applied potential. The main advantage of the pulsed laser compared with continuous light sources (e.g. Ar or Xe lamps) is the improved signal-to-noise ratio of the photocurrent. The pulses used have a width of 10 ns with an intensity of I = 0.3 to 1.5 mJ per pulse. The pulse width on the microsecond timescale is small compared to classical electrochemical methods. The details of the experimental configuration and the electrolytic cell were as described elsewhere [25]. The working electrode was made from massive cylindrical spectroscopically pure niobium rod (Aldrich-Chemie). A stout copper wire

0021-891X/90 $03.00 + .12

was employed as electrical contact. The electrode was fitted into glass tubing of appropriate internal diameter by an epoxy resin, leaving a front area of 0.4 cm^2 to contact the electrolyte. A spiral platinum wire was used as counter electrode and a saturated calomel electrode (SCE) or $Hg/Hg_2SO_4/0.5\,M\ H_2SO_4$ (MSE) as reference electrodes. The measured potentials were then referred to the normal hydrogen electrode (NHE). The electrolytic solutions were prepared using reagents of analytical grade and triply distilled water. All measurements were carried out at a constant temperature of 23° C. The small photocurrents were integrated or averaged and integrated. The resolution was about 50 pA per light pulse. The light source was a dye laser, FL 20001 (Lamda Physik) filled with coumarin 307 (λ_m = 500 nm), rhodamine 6G (λ_m = 581 nm) or PBBO (λ_m = 390 nm) and pumped by an excimer laser. The repetition frequency of the pulse was between 7 and 20 Hz. The electrochemical instrumentation consisted of a Wenking voltage scan generator and a high speed potentiostat. All measurements were performed under potentiostatic control. The cell current and the photocurrent were recorded with an XY_1Y_2 recorder (Linseis, model 181.31.31) or a microcomputer with IEEE 488 interface connected to a multiplexer and a voltmeter (Keithley MUX705, DMM195). Capacitance measurements were carried out using the lock-in technique at a frequency of 1330 Hz. Before each experiment the electrode surface was mechanically polished with diamond spray down to 0.25 μm, and washed first in ethanol, then in triply distilled water in an ultrasonic bath. The passive films were formed galvanostatically at 2.5 mA cm^{-2} to the desired formation voltage. After reaching the desired formation voltage, the current was interrupted and the measurements were carried out immediately.

3. Results and discussion

The rate of formation of oxide film is a function of the anodization potential; a value of 2.1 to 2.5 nm V^{-1} depending on the current density was reported [18]. In contrast to titanium, niobium could be anodized in both nitric acid and sulphuric acid solutions to high voltage (E_F > 100 V) without breakdown [25]. The anodization of niobium in 1 M HNO_3 takes more time than its anodization in 0.5 M H_2SO_4 to the same formation voltage, e.g., for a 9 V layer, it took 43 min in nitric acid and only 5 min in sulphuric acid at the same current density of 2.5 mA cm^{-2}. In all cases, the oxide film acquired a clear interference colour ranging between light yellow (3 V layer), yellowish brown (9 V layer), and bluish brown (> 50 V layer).

Table 1. Donor concentration (N_D) and flat band potential (E_{Fb}) of passivated niobium electrodes in different solutions

Passivating medium	*Test solution*	$N_D(10^{-19}\ cm^{-3})$	$E_{Fb}(mV)$
0.5 M H_2SO_4	0.5 M H_2SO_4	7.83	−175
0.5 M H_2SO_4	1 M HNO_3	6.27	−175
1 M HNO_3	1 M HNO_3	3.63	−175

Formation potential, 3 V (SCE).

The photoelectrochemical behaviour of niobium electrodes passivated in 1 M HNO_3 and 0.5 M H_2SO_4 is illustrated in Fig. 1. Both electrodes were anodized under the same conditions to 3 V with respect to SCE. The two curves presented in Fig. 1 show that the two electrodes had a maximum in the photocharge of the pulse per cm^2 (Q_{Ph}). This maximum is shifted in 1 M HNO_3 about 300 mV cathodic and is slightly smaller than that measured in 0.5 M H_2SO_4 solution. The slight difference in behaviour between the passivated Nb in HNO_3 and that in H_2SO_4 solutions is also reflected in the Mott–Schottky plots corresponding to the capacity measurements obtained with the two kinds of oxide layers. Figure 2 presents the Mott–Schottky plots obtained with an electrode passivated and measured in 0.5 M H_2SO_4, another passivated and measured in 1 M HNO_3, and a third passivated in H_2SO_4 and measured in HNO_3. The corresponding values of the flat band potential and donor concentration are summarized in Table 1.

Unlike titanium [25], the photocharge maximum shown in Fig. 1 is independent of the direction of the voltage sweep, that is, on going from anodic potentials

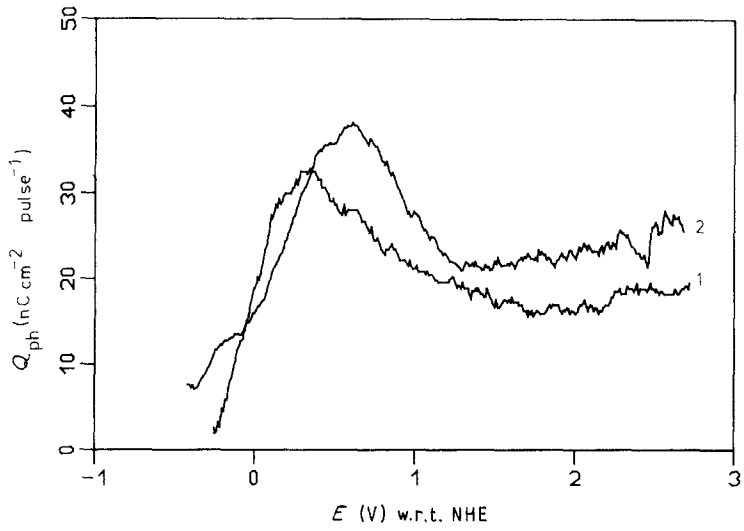

Fig. 1. Photocharge–potential relations of niobium electrode passivated in: (1) 1 M HNO_3 and (2) 0.5 M H_2SO_4 to 3.24 V (NHE), light intensity I = 0.3 mJ cm^{-2} per pulse, λ = 500 nm, scan rate = 10 mV s^{-1}.

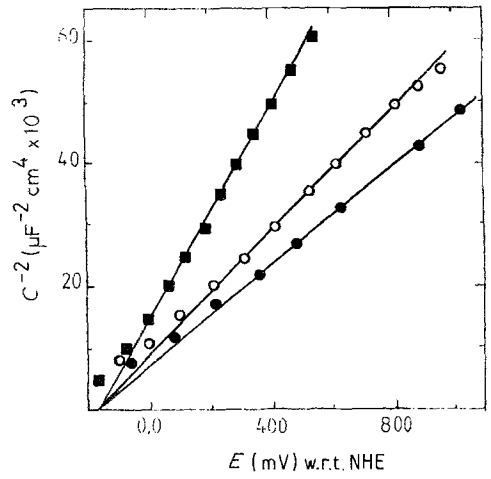

Fig. 2. Mott–Schottky plots of passivated niobium at 2.5 mA cm^{-2} to 3.24 V (NHE): passivated and measured in 0.5 M H_2SO_4 (●); passivated in 0.5 M H_2SO_4, measured in 1 M HNO_3 (○); passivated and measured in 1 M HNO_3 (■).

into the hydrogen evolution, a mixture is present, which is still forming on reversing the scan. The scan rate was 10 mV s^{-1}. If hydrogen is cathodically evolved at the electrode, a second photocharge maximum appears on going from hydrogen evolution (around − 400 mV w.r.t. NHE) to the anodic direction.

The photocharge corresponding to this maximum is a function of the time of hydrogen evolution on the electrode. Figure 3 shows the photocharge–potential behaviour of a niobium electrode passivated in 0.5 M

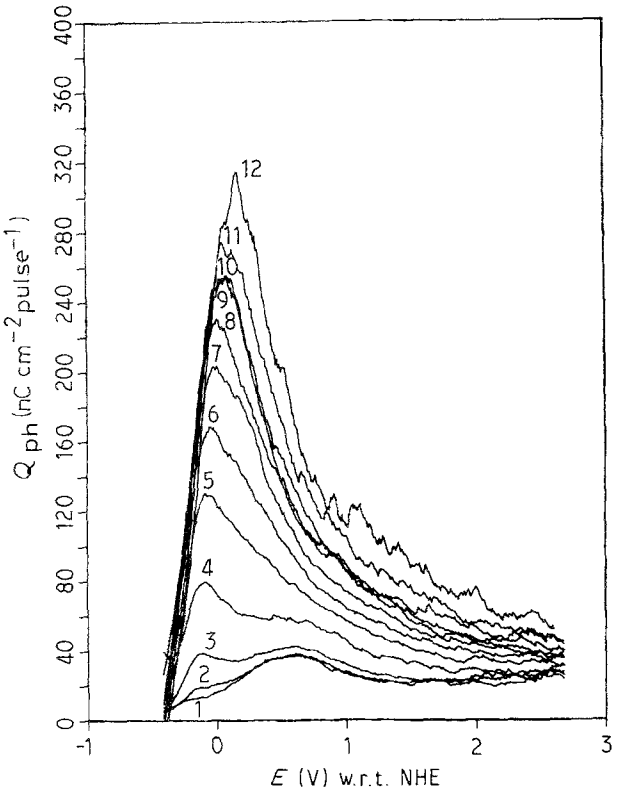

Fig. 3. Photocharge–potential behaviour of passivated niobium electrode in 0.5 M H_2SO_4 to 3.24 V (NHE) after different intervals of cathodic hydrogen evolution (E = 0.3 mJ per pulse, λ = 500 nm): increasing photocharge maximum of H_2 oxidation on the surface from 2 ms to 10 s in steps of 2, 5, 10, 20, 50, 100, 200, 500 ms, 1, 2, 5 and 10 s (from 1 to 12), respectively.

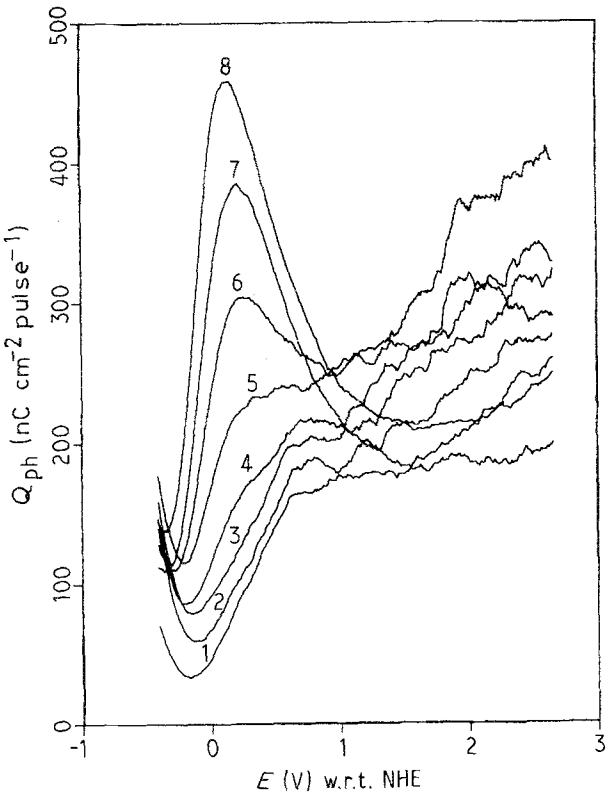

Fig. 4. Photocharge–potential behaviour of 3.24 V passivated Nb-electrode in 0.5 M H_2SO_4 at different time intervals of cathodic hydrogen evolution (E = 0.3 mJ per pulse, λ = 390 nm): increasing photocharge maximum of hydrogen oxidation on the electrode surface in steps of 1, 2, 5, 10, 20, 50, 100 and 200 ms (from 1 to 8), respectively.

H_2SO_4 to 3 V (w.r.t. SCE) after different intervals of cathodic hydrogen evolution ranging between 1 ms and 10 s. The energy of the laser beam was 0.33 mJ per pulse with a wavelength λ of 500 nm. The measurements showed that the photocharge maximum increases as the time of hydrogen evolution on the passivated electrode increases. For comparison, 10 ms of hydrogen evolution gave a photocharge maximum of around 40 mC cm^{-2} per pulse whereas a 10 s hydrogen evolution was accompanied by a maximum of 315 nC cm^{-2} per pulse. Also, the position of the photocharge maximum is shifted towards more positive potentials. The photocharge maximum of the 10 ms hydrogen evolution occurs at around − 120 mV, and that of the 10 s evolution occurs at around + 200 mV. Using laser pulses of shorter wavelengths, namely 390 nm, the photocharge increases: for example, for 20 ms hydrogen evolution a maximum of around 460 nC cm^{-2} per pulse was measured, whereas for the same time of hydrogen evolution using

Table 2. Photocharge and potential of the photocharge maximum corresponding to cathodic hydrogen evolution for 100 ms at the 3 V passivated Nb-electrode in 0.5 M H_2SO_4 at different wavelengths

λ(nm)	*Photocharge (nC cm^{-2} per pulse)*	E_{max} *(mV (NHE))*
581	42	− 160
500	168	− 53
390	386	+ 187

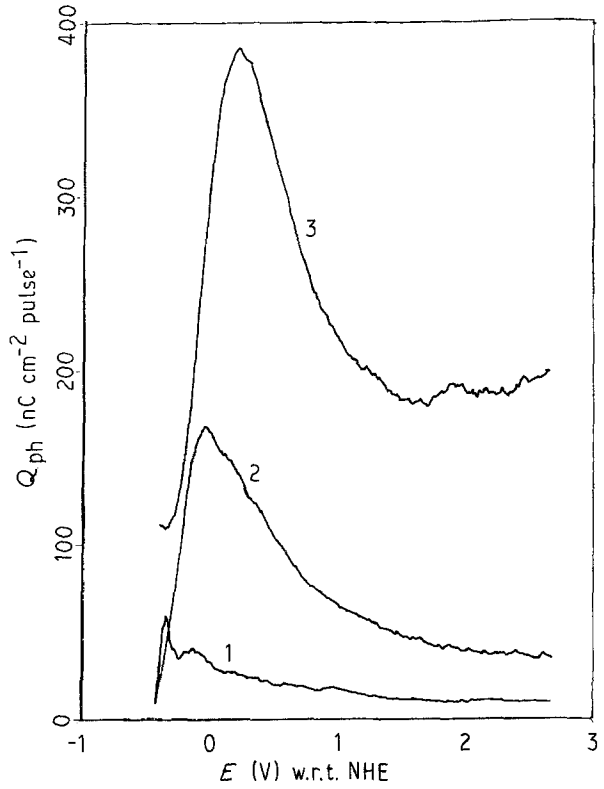

Fig. 5. Effect of the wavelength of the incident laser flash on the photocharge–potential behaviour of a 3.24 V passivated niobium electrode in 1 M H_2SO_4 after cathodic hydrogen evolution of 100 ms (E = 0.3 mJ per pulse): increasing photocharge maximum of hydrogen oxidation on the electrode surface with increasing frequency (λ = 581 (1), 500 (2) and 390 (3) nm, respectively).

a laser beam of λ = 500 nm, a maximum of around 200 nC cm^{-2} per pulse was recorded (cf. Fig. 4). Figure 4 shows also that at higher frequencies the effect of hydrogen evolution in the first few milliseconds (up to 20 ms) is not as pronounced as in the case of low frequencies (compare Fig. 4 with Fig. 3).

The effect of frequency of the incident laser beam on the photocharge–potential behaviour of the passivated Nb-electrode is demonstrated in Fig. 5. Besides the increase in the photocharge corresponding to the maximum, a shift in the potential of that maximum towards anodic potentials with increasing frequency was recorded. The photocharge per cm^2 per pulse and the potential of the maximum at different frequencies of incident laser beam are summarized in Table 2.

The results of photocharge measurements were confirmed by capacity measurements. Figure 6 illustrates the effect of time of the cathodic hydrogen evolution on the capacity–potential behaviour of the passivated Nb-electrode in 0.5 M H_2SO_4 presented as C^{-2} against E relations (Mott–Schottky plots). In this figure, the Mott–Schottky plots exhibit an inflection, that is the plot consists of two parts. The first segment of the plot occurs from the potential of hydrogen evolution up to around + 700 mV (NHE). This part seems to be independent of the time of hydrogen evolution and corresponds to a layer containing higher donor concentration, either from adsorbed hydrogen or as incorporated hydrogen in the oxide layer itself. The donor concentration in this part is about one order of magnitude greater than in the second part ($N_D \simeq$ 2.13 to 2.55 × 10^{20} cm^{-3}) and the flat band potential is about − 240 mV (w.r.t. NHE). The second part of the plot depends on the time of hydrogen evolution. As this increases, the donor concentration increases and the flat band potential is shifted towards more positive values, for example N_D = 1 × 10^{20} cm^{-3} and E_{Fb} = 660 mV for a 10 s evolution of hydrogen on the passive niobium electrode. For 10 ns, values of 3.6 × 10^{19} cm^{-3} for N_D and 570 mV for E_{Fb} were recorded.

The behaviour in 1 M HNO_3 is quite different. The inflection in the Mott–Schottky plot appears only if the time of hydrogen evolution is of the order of seconds, that is $\geqslant$ 1 s. The donor concentration is generally less than in the first part of the layer formed in the H_2SO_4 solution (N_D = 8.2 to 15.0 × 10^9 cm^{-3}) and the flat band potential is more anodic [$E_{FB} \simeq$ − 190 mV]. For a 10 s evolution of hydrogen, the plot exhibits two segments: the first one has a donor concentration of 1.5 × 10^{20} cm^{-3} and E_{Fb} of − 270 mV, whereas the second part has a value of $N_D \simeq$ 1 × 10^{20} cm^{-3} and $E_{Fb} \simeq$ + 235 mV.

The disappearance of the first part in nitric acid solution for small hydrogen evolution times may be explained by the fast oxidation and removal of the hydrogen formed by nitric acid or by the reduction of HNO_3 itself. This process prevents the adsorption or

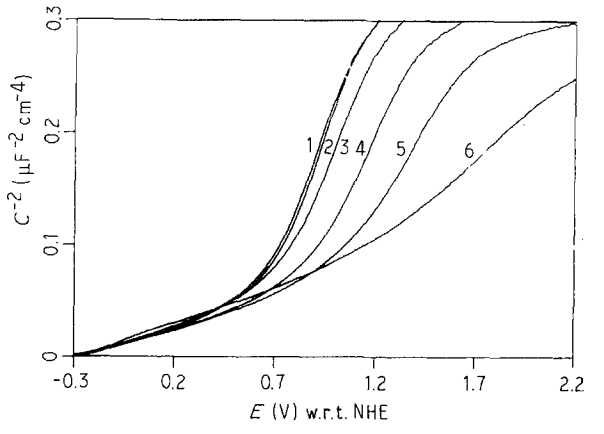

Fig. 6. Mott–Schottky plots of a 3.24 V passivated niobium electrode in 0.5 M H_2SO_4 at different times interval of cathodic hydrogen evolution: (1) 0 ms, (2) 1 ms, (3) 10 ms, (4) 100 ms, (5) 1 s, (6) 10 s.

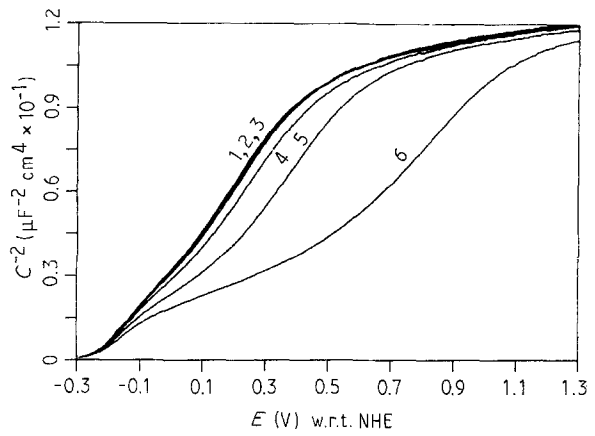

Fig. 7. Mott–Schottky plots of a passivated niobium electrode in 1 M HNO_3 under the same conditions as in Fig. 6.

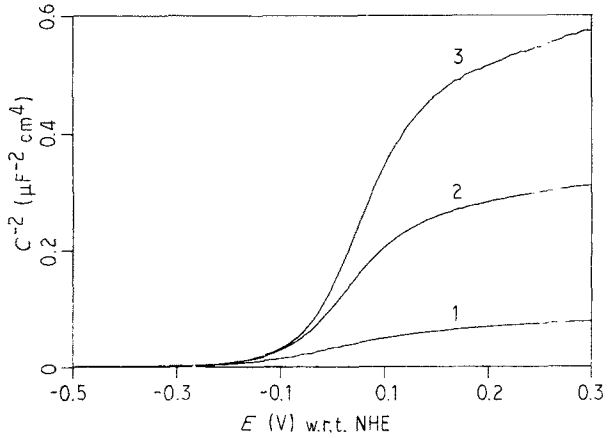

Fig. 8. Effect of the layer thickness on the Mott–Schottky plots of niobium electrode passivated in 0.5 M H_2SO_4 without hydrogen evolution: (1) 3.24 V layer; (2) 6.24 V layer; (3) 9.24 V layer.

incorporation of hydrogen. Hence a more or less unchanged oxide layer is still present. When the time of cathodic hydrogen evolution increases, the amount of hydrogen increases. Consequently, the possibility of incorporation and/or adsorption of hydrogen increases which leads to the appearance of the second segment at more anodic potentials. Because of the anodic oxidation of such incorporated or adsorbed species, a more homogeneous layer similar to the second part observed in H_2SO_4 solution will be present (cf. Fig. 6).

The effect of the oxide film thickness on its electrochemical properties is illustrated in Figs 8 and 9. In Fig. 8, the Mott–Schottky plots of niobium electrodes passivated in 0.5 M H_2SO_4 to different anodization potentials, namely 3.0, 6.0 and 9.0 V w.r.t. SCE, are shown. In order to be sure that the passive layer is not contaminated with hydrogen, the electrode capacity was measured from +3.0 to −0.4 V (w.r.t. SCE). The Mott–Schottky plots shown in Fig. 8 are dependent on the layer thickness. The donor concentration decreases as the layer thickness increases (N_D = 6.8×10^{19} cm^{-3} for a 3 V layer and 0.6×10^{19} cm^{-3} for a 9 V layer, respectively). This may be due to the increased stoichiometry with increasing thickness with layers formed under galvanostatic control at low current densities (2.5 mA cm^{-2}). If hydrogen is formed

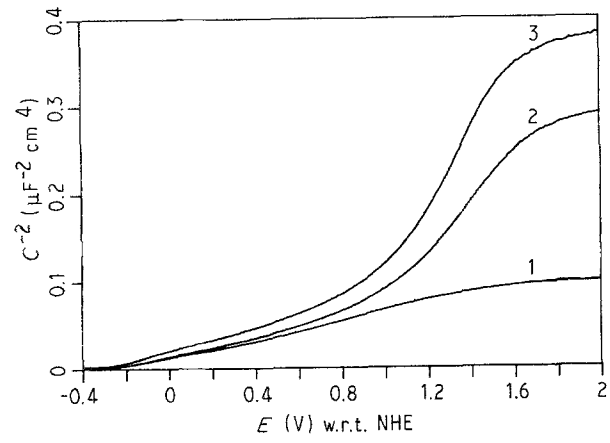

Fig. 9. The same as in Fig. 8, but after cathodic hydrogen evolution for 1 s.

cathodically, the capacity–potential behaviour of the electrode changes (Fig. 9). The two parts of the Mott–Schottky plots become clear. The second part is more affected by the film thickness than the first one. The first part in this case has a flat band potential E_{Fb} = −240 mV and a donor concentration of 2.5×10^{20} cm^{-3}. On the other hand, the donor concentration of the second part decreases as the film thickness increases (N_D = 2.2×10^{20} and 0.27×10^{20} cm^{-3} for a 3 V and 9 V layer, respectively). These values are inconsistent with the values obtained from Fig. 8 in 0.5 M H_2SO_4 solution.

4. Conclusions

(1) The electrochemical and photoelectrochemical behaviour of passivated niobium in nitric acid is slightly different from its behaviour in sulphuric acid.

(2) The cathodic evolution of hydrogen on passivated niobium surface changes the characteristics of the passive film. As the time of hydrogen evolution increases, the amount of adsorbed or incorporated hydrogen increases and a change in the characteristics of the passive layer occurs. This change is reflected in the extrapolated values of the flat band potential and donor concentration. The maximum of the photocharge obtained with the increased time of the cathodic hydrogen evolution can be taken as a measure of the amount of adsorbed hydrogen.

Acknowledgement

The author thanks Professor Dr W. J. Plieth for invaluable discussions and Mr A. Felska for his help with the photocharge measurements. Financial support from the Alexander von Humboldt-Stiftung and the Free University of Berlin is gratefully acknowledged.

References

[1] O. De Nora, *Chem. Ing. Tech.* **42** (1970) 222.
[2] S. Trasatti, 'Electrodes of Conductive Metallic Oxides', Part B, Elsevier, Amsterdam (1980) Chap. 11.
[3] L. Young, 'Anodic Oxide Films', Academic, London (1961).
[4] M. J. Joncich and L. S. Steward, *J. Electrochem. Soc.* **112** (1965) 717.
[5] M. Pourbaix, 'Atlas of Electrochemical Equilibria in Aqueous Solutions', Pergamon (1966).
[6] D. Piron and K. Nobe, *Corros. NACE* **25** (1969) 67.
[7] K. E. Heusler, *Metallik* **61** (1970) 828.
[8] A. D. Davydov, V. D. Kashcheev and A. N. Kamkin, *Electrokhimiya* **8** (1972) 282.
[9] S. Iseki, K. Ohashi and S. Nagaura, *Electrochim. Acta* **17** (1972) 2239.
[10] O. A. Omel'chenko and Ya. S. Gorodetskii, *Zasch. Met.* **11** (1975) 466.
[11] R. Badar, G. Bouyssoux and M. Romand, *Mater. Res. Bull.* **11** (1976) 525.
[12] A. Ya. Shatalov, T. P. Bondareva and L. E. Tsygantaus, *J. Appl. Chem. USSR* **36** (1963) 561.
[13] M. S. El Basiouny, A. M. Bekheet and A. G. Gad-Allah, *Corros. NACE* **40** (1984) 116.
[14] W. A. Badawy, A. G. Gad-Allah and H. H. Rehan, *J. Appl. Electrochem.* **17** (1987) 559.
[15] D. Stutzle and K. E. Heusler, *Z. Phys. Chem. Neue Folge* **65** (1969) 201.
[16] D. A. Vermilyea, 'Advances in Electrochemistry and Elec-

trochemical Engineering' (edited by P. Delahay), Vol. 3, Interscience, New York (1963) Chap. 3.
[17] W. S. Goruk, L. Young and F. G. R. Zobel, 'Modern Aspects of Electrochemistry' (edited by J. O.'M. Bockris), No. 4, Plenum, New York (1966) Chap. 3.
[18] F. Di Quarto, C. Sunseri and S. Piazza, *Ber. Bunsenges. Phys. Chem.* **90** (1986) 549, **91** (1987) 437.
[19]. A. J. Schrijner and A. Middelhoek, *J. Electrochem. Soc.* **111** (1964) 1167.
[20] W. Schmickler and J. W. Schultze, 'Modern Aspects of Electrochemistry' (edited by J. O.'M. Bockris, B. E. Conway and R. E. White), No. 17, Plenum, New York (1986) Chap. 5.
[21] S. R. Morrison, 'Electrochemistry at Semiconductor and Oxidized Metal Electrodes', Plenum, New York (1980).
[22] J. R. Narayanan, B. Viswanathan, R. P. Viswanath and T. K. Varadarajan, *Ind. J. Technol.* **19** (1981) 449.
[23] G. Marx, A. Bestanpouri, R. Droste, W. Erben, W. Schonemann and D. Wegen, *J. Less Common Metals* **121** (1986) 507.
[24] A. Felske and W. J. Plieth, *J. Opt. Soc. Am. B* **3** (1986) 815.
[25] A. Felske, W. A. Badawy and W. J. Plieth, *J. Electrochem. Soc.* in press.